On the Diversity Order of BICM-OFDM in Doubly Selective Fading Channels

Hsin-De Lin, *Student Member, IEEE*, and
Tzu-Hsien Sang, *Member, IEEE*

***Abstract*—Bit-interleaved coded modulation with orthogonal frequency-division multiplexing (BICM-OFDM) is an attractive approach to achieve time and frequency diversity. Remarkable diversity gain can be obtained when the channel is doubly selective fading. In this paper, the asymptotic diversity orders of BICM-OFDM systems in doubly selective fading channels for both single-input–single-output (SISO) and multiple-input–multiple-output (MIMO) cases are derived. In addition, the system bit-error-rate (BER) behavior in practical situations with moderate signal-to-noise ratios (SNRs) is also investigated. In the SISO case, the diversity order depends on the rank of the channel correlation matrix. Therefore, the channel variations induced by fast fading contribute to improving diversity. In the MIMO case, the diversity order can be further increased when factors such as cyclic delays or phase rolls are introduced. Simulations are provided to verify the analysis.**

***Index Terms*—Bit-interleaved coded modulation (BICM), diversity order, doubly selective fading channel, orthogonal frequency-division multiplexing (OFDM).**

I. Introduction

Wireless communication faces the ever-present demand for higher data rates with more efficient spectrum usage while maintaining good quality of service in high motion speeds. Two transmission techniques that are very popular in that regard are bit-interleaved coded modulation (BICM) and orthogonal frequency-division multiplexing (OFDM). BICM counters fading channels by spreading code-word bits in time to exploit the time diversity available in the time-varying channel response [1], [2], whereas OFDM claims high bandwidth efficiency and simplicity in receiver design.

Doubly selective fading channels in many situations have been viewed as the cause of severe channel impairments, e.g., the inter-carrier interference (ICI), and many techniques, such as ICI-canceling equalizers, have been developed to mitigate the problem [3]. However, it is also considered as a potential source of time and frequency diversity, which may enhance the system performance [4]–[6]. Pioneering work by Ma and Giannakis [7] considers the maximum diversity order over doubly selective channels for general block transmission systems without forward error correction (FEC). Recent papers have started investigating time diversity for coded systems. Huang *et al*. [8] and Liu and Fitz [9] have reported that, in simulations, the performance of BICM-OFDM systems is improved when the channel is fast fading. In [10], the diversity order of BICM-OFDM systems in frequency selective, but not doubly selective, fading channels is analyzed.

This paper aims to extend these pioneering works and provide an analytic study of the diversity order of BICM-OFDM systems over doubly selective fading channels. First, we derive the asymptotic diversity order of BICM-OFDM systems by studying the role of the channel autocorrelation matrix in rank analysis of the typical derivation of diversity order. Second, the effect of significant eigenvalues of the channel autocorrelation matrix and the diversity order in realistic situations with moderate SNRs are examined by studying the channel autocorrelation function (ACF) and its Fourier dual. Finally, our analysis framework is extended to multiple-input–multiple-output (MIMO) cases while incorporating more diversity techniques, such as cyclic delay diversity (CDD) and phase-roll diversity (PRD) [11]. This MIMO extension can also be applied in a distributed fashion, for example, in cooperative communications [12].

Manuscript received April 30, 2011; revised May 3, 2012, September 17, 2012, and November 26, 2012; accepted December 2, 2012. Date of publication December 19, 2012; date of current version May 8, 2013. This work was supported by the National Science Council of the Republic of China under Grant NSC 101-2220-E-009-003, Grant NSC 101-2220-E-009-058, and Grant NSC 101-2219-E-009-021. The review of this paper was coordinated by Prof. M. Uysal.

The authors are with the Department of Electronics Engineering and Institute of Electronics, National Chiao Tung University, Hsinchu 300, Taiwan (e-mail: good.ee92g@nctu.edu.tw; tzuhsien54120@faculty.nctu.edu.tw).

Color versions of one or more of the figures in this paper are available online at http://ieeexplore.ieee.org.

Digital Object Identifier 10.1109/TVT.2012.2235091

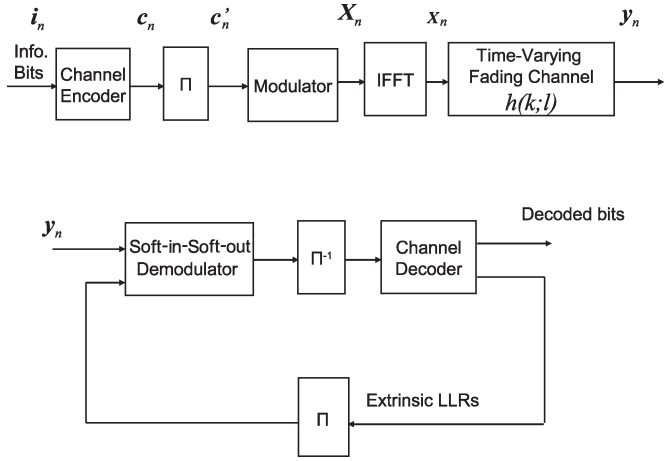

Fig. 1. Block diagram of the transmitter and the receiver of the considered system. Soft-input–soft-output demodulator consists of the ICI equalization such as the feedback canceler [8] and the demapper.

II. Diversity Order Analysis

A. System Model

A block diagram of the BICM-OFDM system under study is shown in Fig. 1. Information bits $\boldsymbol{i}_n$ are first encoded by a channel encoder, and the coded bits $\boldsymbol{c}_n \in \mathcal{C}$ are passed to interleaver Π, where $\mathcal{C}$ is the set of all possible code words. The interleaved bits $\boldsymbol{c}'_n$ are divided into P blocks and modulated using quadrature-amplitude modulation or phase-shift keying (PSK), where γ bits are mapped into one of the total 2^γ constellation points. Finally, an N-point inverse discrete Fourier transform generates the transmitted OFDM signal $\mathbf{x}_n$. The size of the interleaver is γNP bits. Note that the encoded bits are interleaved across several OFDM symbols as in [8] (which calls it time–frequency interleaving). Considering the time-varying dispersive channels, the sampled baseband equivalent received signal $y_p(k)$ of the pth OFDM symbol is

$$y_p(k) = \sum_{l=0}^{L-1} h_p(k;l)x_p(k-l) + w_p(k) \tag{1}$$

where $h_p(k;l)$ represents the lth delay path of the multipath Rayleigh fading channel at the kth sampling instant of the pth OFDM symbol with $E[\sum_{l=0}^{L-1}|h_p(k;l)|^2] = 1$, L is the number of multipaths, $x_p(k)$ is the transmitted signal, and $w_p(k)$ is the additive white Gaussian noise. The channel $\{h_p(k;l)\}$ is assumed to be wide-sense stationary uncorrelated scattering. The autocorrelation function (ACF) of the channel in time for the lth path is defined as $r(m) = E[h_p(k;l)h^*_{p+m}(k;l)]$.

Assume that the cyclic prefix (CP) is long enough to prevent intersymbol interference and that the synchronization is perfect. The received symbol in the frequency domain after CP removal is

$$\boldsymbol{y}_p = \boldsymbol{F}\boldsymbol{H}_p\boldsymbol{F}^H\boldsymbol{x}_p + \boldsymbol{w}_p \triangleq \boldsymbol{G}_p\boldsymbol{x}_p + \boldsymbol{w}_p,\ p = 1, 2, \ldots, P, \quad (2)$$

where $\boldsymbol{y}_p = [Y(N_p), Y(N_p+1), \ldots, Y(N_p+N-1)]^T \in \mathbb{C}^{N\times 1}$ is the frequency-domain signal after discrete Fourier transform (DFT); $N_p = (p-1)N$ marks the starting point of the pth OFDM symbol; $[\boldsymbol{F}]_{k,n} = (1/\sqrt{N})e^{-j2\pi nk/N}$ is the (k,n)th element in the DFT matrix $\boldsymbol{F}$; $\boldsymbol{x}_p = [X(N_p), X(N_p+1), \ldots, X(N_p+N-1)]^T \in \mathbb{C}^{N\times 1}$ is the transmitted coded signal in the frequency domain with the average power normalized to 1; $\boldsymbol{w}_p = [W(N_p), W(N_p+1), \ldots, W(N_p+N-1)]^T \in \mathbb{C}^{N\times 1}$ represents the noise; and $\boldsymbol{H}_p \in \mathbb{C}^{N\times N}$ is the channel impulse response (CIR) matrix given by

$$[\boldsymbol{H}_p]_{i,j} = h_p\left(i; (i-j) \bmod N\right), \quad 1,\ j = 0, 1, \ldots, N-1. \quad (3)$$

Note that the CIR $h_p(k;l)$ is zero when $l \le 0$ or $l \ge L-1$. The off-diagonal terms in $\boldsymbol{G}_p$ are the ICI coefficients, where the $(r,\ s)$th element can be expressed as

$$[\boldsymbol{G}_p]_{r,s} = \frac{1}{N}\sum_{k=0}^{N-1}\sum_{l=0}^{L-1} h_p(k;l)\exp\left(j2\pi k(s-r)/N\right) \times \exp(-j2\pi sl/N). \quad (4)$$

The channel matrix $\boldsymbol{G}_p$ can be decomposed as $\boldsymbol{G}_p = \boldsymbol{G}_p^d + \boldsymbol{G}_p^o$, where $\boldsymbol{G}_p^d$ contains the diagonal terms of $\boldsymbol{G}_p$, and $\boldsymbol{G}_p^o$ consists all the off-diagonal terms of $\boldsymbol{G}_p$. Note that $\boldsymbol{G}_p^d$ corresponds to the DFT of $\tilde{\boldsymbol{h}}_p = [\tilde{h}_p(0), \ldots, \tilde{h}_p(L-1)]^T$, the *averaged* CIR in the pth OFDM symbol, i.e., $\tilde{h}_p(l) = (1/N)\sum_{k=0}^{N-1} h_p(k,l)$. Meanwhile $\boldsymbol{G}_p^o$ contributes to ICI terms. We can rewrite (2) as

$$\boldsymbol{y}_p = \boldsymbol{G}_p^d\boldsymbol{x}_p + \boldsymbol{G}_p^o\boldsymbol{x}_p + \boldsymbol{w}_p = \mathrm{diag}(\boldsymbol{x}_p)\boldsymbol{F}_{N\times L}\tilde{\boldsymbol{h}}_p + \boldsymbol{z}_p \quad (5)$$

where $\boldsymbol{F}_{N\times L}$ is an $N\times L$ matrix composed of the first L columns of $\boldsymbol{F}$, and $\boldsymbol{z}_p$ denotes the interference-plus-noise terms.

The variation of doubly selective fading channels within one or across several OFDM symbols can provide some benefits. The intrasymbol channel variation also causes ICI. It has been observed that the diversity order slightly increases if ICI is utilized at the receiver [4]–[6], [9], but the high complexity remains a concern. In this paper, we focus on the much more pronounced benefit provided by the intersymbol channel variation, assuming that ICI is handled by simple techniques such as the decision-feedback canceler [8] with FEC to improve the decision accuracy. In particular, we assume that any *residual* ICI will not ruin the possible diversity gain provided by intersymbol channel variation. This assumption is reasonable even if the normalized Doppler frequency f_dT_S (T_S is one OFDM symbol duration) is as high as 0.1, about which many ICI mitigation methods can reach around 30 dB of signal-to-interference ratio without the help of FEC [13], [14]. As a result, the error floor due to residual ICI will not kick in until a very high SNR.

With this focus in mind, the stacked received signal $\boldsymbol{y} = [\boldsymbol{y}_1^T, \boldsymbol{y}_2^T, \ldots, \boldsymbol{y}_P^T]^T$ can be given as

$$\boldsymbol{y} = \boldsymbol{X}(\boldsymbol{I}_P \otimes \boldsymbol{F}_{N\times L})\boldsymbol{h} + \boldsymbol{z} \triangleq \boldsymbol{X}\boldsymbol{h}_{\mathrm{eq}} + \boldsymbol{z} \quad (6)$$

in which $\boldsymbol{h}_{\mathrm{eq}} \triangleq (\boldsymbol{I}_P \otimes \boldsymbol{F}_{N\times L})\boldsymbol{h}$, $\boldsymbol{I}_P$ is a $P\times P$ identity matrix; $\otimes$ denotes the Kronecker product; $\boldsymbol{h}$ is a length-PL vector defined as $\boldsymbol{h} = [\tilde{\boldsymbol{h}}_1^T, \tilde{\boldsymbol{h}}_2^T, \ldots, \tilde{\boldsymbol{h}}_P^T]^T$; $\boldsymbol{X}$ is a $PN\times PN$ diagonal data signal matrix given by $\boldsymbol{X} = \mathrm{diag}(X(0), \ldots, X(N-1), X(N), \ldots, X(2N-1), \ldots, X(PN-1))$; and $\boldsymbol{z}$ is a $PN\times 1$ noise vector representing the residual ICI plus noise.

B. Asymptotic Analysis

Here, we derive the asymptotic diversity order of BICM-OFDM by first bounding the pairwise error probability (PEP). Let $\boldsymbol{X}$ be the coded transmit signal corresponding to code word $\boldsymbol{c}$ and $\hat{\boldsymbol{X}}$ be the detected signal corresponding to code word $\hat{\boldsymbol{c}}$, where $\boldsymbol{c} \ne \hat{\boldsymbol{c}}$. To gain diversity, we adopt the assumption in [10] that the interleaver can disperse d consecutive coded bits to different symbols and onto different OFDM subcarriers, whereas d bits cover the span of consecutive trellis branches on which d_{free} distinct bits of any two code words occur. The assumption can be satisfied by practical interleavers, for instance, the block interleaver of IEEE 802.11a [15]. Assume that $\boldsymbol{z}$ is complex Gaussian distributed with zero mean and variance N_0. Evoke the maximum-likelihood (ML) decision rule, and the conditional error probability $P(\boldsymbol{c} \to \hat{\boldsymbol{c}}|\boldsymbol{h})$ is $P(\|\boldsymbol{z}\|^2 \ge \|\boldsymbol{z} + (\boldsymbol{X} - \hat{\boldsymbol{X}})\boldsymbol{h}_{\mathrm{eq}}\|^2|\boldsymbol{h})$. It can be expressed by the Q-function as

$$Q\left(\frac{\left\|(\boldsymbol{X}-\hat{\boldsymbol{X}})\boldsymbol{h}_{\mathrm{eq}}\right\|^2}{\sqrt{2N_0\left\|(\boldsymbol{X}-\hat{\boldsymbol{X}})\boldsymbol{h}_{\mathrm{eq}}\right\|^2}}\right) = Q\left(\sqrt{\frac{1}{2N_0}}\left\|(\boldsymbol{X}-\hat{\boldsymbol{X}})\boldsymbol{h}_{\mathrm{eq}}\right\|\right) \quad (7)$$

where $Q(x) = (1/\sqrt{2\pi})\int_x^\infty e^{-(y^2/2)}dy$.

The PEP is obtained by ensemble averaging, i.e.,

$$\begin{aligned} P(\boldsymbol{c}\to\hat{\boldsymbol{c}}) &= E\left[Q\left(\sqrt{\frac{1}{2N_0}}\left\|(\boldsymbol{X}-\hat{\boldsymbol{X}})\boldsymbol{h}_{\mathrm{eq}}\right\|\right)\right] \\ &= E\left[Q\left(\sqrt{\frac{\mathrm{SNR}\cdot\boldsymbol{h}_{\mathrm{eq}}^H\boldsymbol{D}^H\boldsymbol{D}\boldsymbol{h}_{\mathrm{eq}}}{2}}\right)\right] \end{aligned} \quad (8)$$

where $\mathrm{SNR} = 1/N_0$ since the average power of channel and transmitted signal are normalized to 1, and $\boldsymbol{D} = \boldsymbol{X} - \hat{\boldsymbol{X}}$ is the coded symbol difference matrix. According to the assumption of the interleaver, at least d_{free} nonzero terms exist in $\boldsymbol{D}$ [10]. In the following, we consider the worst case that only d_{free} terms are nonzero in $\boldsymbol{D}$, and each of these terms has Euclidean distance $d_{\min}$. Note that the parameters of BICM-OFDM are usually chosen as $N \ge L$ and $N \ge d_{\mathrm{free}}$.

A typical PEP analysis such as those in [10] and [16] assumes that the vector $\boldsymbol{h}_{\mathrm{eq}}$ has independent elements and the rank analysis is focused on the term $\boldsymbol{D}^H\boldsymbol{D}$. Here, however, the correlation of channels over several OFDM symbols needs to be considered. We adopt the approach in [7] to extract the statistical independent components in $\boldsymbol{h}_{\mathrm{eq}}$, which are considered as the source of diversity. After this extraction, the usual PEP analysis can proceed.

Assume the Kronecker model [11], [17], [18] for the channel, i.e., the channel autocorrelation matrix can be decoupled as

$$\boldsymbol{R} = E[\boldsymbol{h}\boldsymbol{h}^H] = \boldsymbol{\Phi}_T \otimes \boldsymbol{\Phi}_L \quad (9)$$

where $\boldsymbol{\Phi}_T$ is the $P\times P$ time autocorrelation matrix constructed by stacking the windowed ACFs, i.e., the kth row $[\boldsymbol{\Phi}_T]_{k,1:P} = [r(1-k), r(2-k), \ldots, r(P-k)]$. $\boldsymbol{\Phi}_L$ is the autocorrelation matrix of the $L\times L$ path gain and constructed as a diagonal matrix $\mathrm{diag}(\sigma_0^2, \sigma_1^2, \ldots, \sigma_{L-1}^2)$ due to the uncorrelated scattering assumption, where σ_l^2 denotes the power of the lth path.

The rank of $\boldsymbol{R}$ can be evaluated through [19, Fact 7.4.20]

$$\begin{aligned} \mathrm{rank}(\boldsymbol{R}) &= \mathrm{rank}(\boldsymbol{\Phi}_T \otimes \boldsymbol{\Phi}_L) \\ &= \mathrm{rank}(\boldsymbol{\Phi}_T) \times \mathrm{rank}(\boldsymbol{\Phi}_L) = r_T \times L \end{aligned} \quad (10)$$

where r_T and L are the ranks of $\boldsymbol{\Phi}_T$ and $\boldsymbol{\Phi}_L$, respectively. Note that $r_T \times L$ is bounded by $P\times L$. The autocorrelation matrix of $\boldsymbol{h}_{\mathrm{eq}}$ is $\boldsymbol{R}_{\mathrm{eq}} = E[\boldsymbol{h}_{\mathrm{eq}}\boldsymbol{h}_{\mathrm{eq}}^H] = (\boldsymbol{I}_P \otimes \boldsymbol{F}_{N\times L})E[\boldsymbol{h}\boldsymbol{h}^H](\boldsymbol{I}_P \otimes \boldsymbol{F}_{N\times L})^H = (\boldsymbol{I}_P \otimes \boldsymbol{F}_{N\times L})\boldsymbol{R}(\boldsymbol{I}_P \otimes \boldsymbol{F}_{N\times L})^H$. Since $\boldsymbol{F}_{N\times L}$ has full rank L,

matrix $(\boldsymbol{I}_P \otimes \boldsymbol{F}_{N\times L})$ also has full rank PL. Therefore, by the rank property of matrix products [19, Prop. 2.6.2],[1] the rank of $\boldsymbol{R}_{\rm eq}$ is

$$\begin{aligned}\text{rank}(\boldsymbol{R}_{\rm eq}) &= \text{rank}\left((\boldsymbol{I}_P \otimes \boldsymbol{F}_{N\times L})\boldsymbol{R}(\boldsymbol{I}_P \otimes \boldsymbol{F}_{N\times L})^H\right)\\ &= \text{rank}(\boldsymbol{R}) = r_T \times L. \end{aligned} \tag{11}$$

The eigenvalue decomposition is used to extract the statistically independent components in $\boldsymbol{h}_{\rm eq}$. Consider $\boldsymbol{R}_{\rm eq} = \boldsymbol{V}\boldsymbol{\Sigma}_h\boldsymbol{V}^H$, where $\boldsymbol{V}$ is a $PN \times r_T L$ matrix satisfying $\boldsymbol{V}^H\boldsymbol{V} = \boldsymbol{I}_{r_T L}$ and $\boldsymbol{\Sigma}_h = \text{diag}(\xi_1^2, \ldots, \xi_{r_T L}^2)$. In the following analysis, $\boldsymbol{h}_{\rm eq}$ is substituted by $\boldsymbol{V}\boldsymbol{\Sigma}_h^{1/2}\bar{\boldsymbol{h}}_{\rm eq}$, where $\bar{\boldsymbol{h}}_{\rm eq}$ is the $r_T L \times 1$ normalized equivalent channel vector containing independent and identically distributed (i.i.d.) zero-mean complex Gaussian random variables with unit variance. It can be shown that the PEP is not affected by this substitution since $\boldsymbol{h}_{\rm eq}$ and $\boldsymbol{V}\boldsymbol{\Sigma}_h^{1/2}\bar{\boldsymbol{h}}_{\rm eq}$ have identical distributions, which is known as the isotropy property of the standard Gaussian random vector.

The term $\boldsymbol{h}_{\rm eq}^H\boldsymbol{D}^H\boldsymbol{D}\boldsymbol{h}_{\rm eq}$ in (8) now becomes $\bar{\boldsymbol{h}}_{\rm eq}^H(\boldsymbol{\Sigma}_h^{1/2})^H\boldsymbol{V}^H\boldsymbol{D}^H\boldsymbol{D}\boldsymbol{V}\boldsymbol{\Sigma}_h^{1/2}\bar{\boldsymbol{h}}_{\rm eq}$ in which the central part $(\boldsymbol{\Sigma}_h^{1/2})^H\boldsymbol{V}^H\boldsymbol{D}^H\boldsymbol{D}\boldsymbol{V}\boldsymbol{\Sigma}_h^{1/2}$ is a Hermitian matrix and can be diagonalized as $(\boldsymbol{\Sigma}_h^{1/2})^H\boldsymbol{V}^H\boldsymbol{D}^H\boldsymbol{D}\boldsymbol{V}\boldsymbol{\Sigma}_h^{1/2} = \boldsymbol{U}\boldsymbol{\Lambda}\boldsymbol{U}^H$, where $\boldsymbol{U}$ is unitary, r_{TV} is its rank, and $\boldsymbol{\Lambda} = \text{diag}\{\lambda_1, \ldots, \lambda_{r_{TV}}\}$ contains the eigenvalues. Moreover, define $\breve{\boldsymbol{h}} = \boldsymbol{U}^H\bar{\boldsymbol{h}}_{\rm eq}$, and notice that $\breve{\boldsymbol{h}}$ is i.i.d. complex Gaussian with zero mean and unit variance since $\boldsymbol{U}$ is unitary. Equation (8) becomes

$$\begin{aligned}P(\boldsymbol{c}\to\hat{\boldsymbol{c}}) &= E\left[Q\left(\sqrt{\frac{\text{SNR}\cdot\breve{\boldsymbol{h}}^H\boldsymbol{\Lambda}\breve{\boldsymbol{h}}}{2}}\right)\right]\\ &= E\left[Q\left(\sqrt{\frac{\text{SNR}}{2}\sum_{n=1}^{r_{TV}}\lambda_n|\breve{h}_n|^2}\right)\right]\end{aligned} \tag{12}$$

where $\breve{h}_n$ is the nth element in $\breve{\boldsymbol{h}}$, and $|\breve{h}_n|$ is Rayleigh distributed. The PEP is bounded by [16]

$$\begin{aligned}P(\boldsymbol{c}\to\hat{\boldsymbol{c}}) &\le E\left[\exp\left(-\frac{\text{SNR}}{4}\sum_{n=1}^{r_{TV}}\lambda_n|\breve{h}_n|^2\right)\right]\\ &= \frac{1}{\prod_{n=1}^{r_{TV}}[1+(\lambda_n\text{SNR}/4)]}.\end{aligned} \tag{13}$$

When SNR is large enough, the bound in (13) can be further simplified to

$$P(\boldsymbol{c}\to\hat{\boldsymbol{c}}) \le \left(\prod_{n=1}^{r_{TV}}\lambda_n\right)^{-1}\left(\frac{\text{SNR}}{4}\right)^{-r_{TV}}. \tag{14}$$

In addition, it follows that the asymptotic diversity order is r_{TV}. As for the value of r_{TV}, since $\boldsymbol{V}\boldsymbol{\Sigma}_h^{1/2}$ has rank $r_T L$ and the diagonal matrix $\boldsymbol{D}$ has rank $d_{\rm free}$, it follows that $r_{TV} \le \min(r_T L, d_{\rm free})$, i.e., the maximum asymptotic diversity order is no larger than $\min(r_T L, d_{\rm free})$.

[1]Reference [19, Prop. 2.6.2] states the following: Let $\boldsymbol{A} \in \mathbb{C}^{n\times m}$, and let $\boldsymbol{C} \in \mathbb{C}^{k\times n}$ be left invertible (or equivalently, $\text{rank}(\boldsymbol{C}) = n$) and $\boldsymbol{B} \in \mathbb{C}^{m\times l}$ be right invertible (or equivalently, $\text{rank}(\boldsymbol{B}) = m$); then, $\text{rank}(\boldsymbol{A}) = \text{rank}(\boldsymbol{C}\boldsymbol{A}) = \text{rank}(\boldsymbol{A}\boldsymbol{B})$. It is straightforward that $\text{rank}(\boldsymbol{C}\boldsymbol{A}\boldsymbol{B}) = \text{rank}(\boldsymbol{A})$. Since $\text{rank}(\boldsymbol{I}_P \otimes \boldsymbol{F}_{N\times L}) = \text{rank}((\boldsymbol{I}_P \otimes \boldsymbol{F}_{N\times L})^H) = PL$, (11) can be obtained by designating $\boldsymbol{C} = (\boldsymbol{I}_P \otimes \boldsymbol{F}_{N\times L})$, $\boldsymbol{A} = \boldsymbol{R}$, and $\boldsymbol{B} = (\boldsymbol{I}_P \otimes \boldsymbol{F}_{N\times L})^H$.

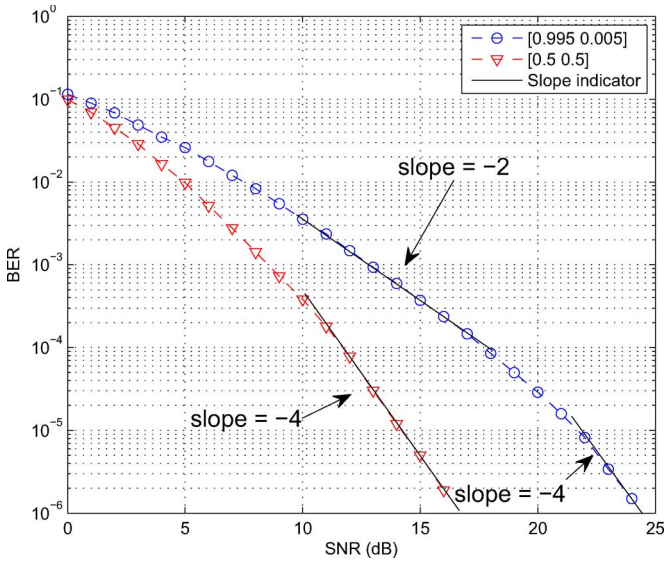

Fig. 2. BER performance with 8-PSK modulation under two-multipath $(L = 2)$ Rayleigh block fading channels with two different path-gain distributions. The DFT size is 64, $P = 2$, and a rate-1/2 convolutional code with the generator polynomial [133; 171] $(d_{\rm free} = 10)$ is adopted. 10^5 channel realizations are simulated.

C. Practical Diversity Gains

Next, we consider the slope of the BER curve that is observed in more *realistic situations*. The full slope of $r_{TV} = \min(r_T L, d_{\rm free})$ from asymptotic analysis is achieved when SNR approaches infinity. In practical situations, smaller eigenvalues of $\boldsymbol{R}_{\rm eq}$ may not have the opportunity to contribute to steepening the slope before the effect of other impairments, such as residual ICI, kicks in. As a result, the actual slope that is observed at moderate SNR would not be as large as the asymptotic slope. A similar phenomenon caused by dominant eigenvalues in the context of channel estimation has also been reported [20].

Simulations are conducted to demonstrate the effect of the relative sizes of eigenvalues on the observed slope. Consider a BICM-OFDM system over a block fading channel. Here, we did not use doubly selective fading channels because the magnitudes of eigenvalues need to be controlled to show their effects, and it is very difficult to do so for a doubly selective fading channel, whereas in a block fading channel, it can be easily done by setting the path gains. Fig. 2 shows two BER curves under two-multipath $(L = 2)$ Rayleigh block fading channel with two different path gain settings. The system uses 8-PSK modulation, the DFT size is 64, $P = 2$, and a rate-1/2 convolutional code with the generator polynomial [133;171] $(d_{\rm free} = 10)$ is adopted such that the diversity order is not limited by $d_{\rm free}$. 10^5 channel realizations are simulated. Two settings of eigenvalues of $\boldsymbol{\Phi}_L$ are used: The first consists of (0.995, 0.05), and the second consists of (0.5, 0.5). The full slope is -4 for both cases, but for the first setting, we expect the slope will only reach -2 when the SNR is moderate since only one eigenvalue is significant. As shown in Fig. 2, in the SNR range from 10 to 20 dB, the slopes are -2 and -4, respectively, and the first setting's slope does not reach -4 until around SNR $= 25$ dB.

The relation between the practical diversity order and the channel ACF can be further expounded. Consider the number of significant eigenvalues of $\boldsymbol{R}_{\rm eq}$ in (11). Since $\boldsymbol{R}_{\rm eq}$ can be approximated to be circulant when N is large, its eigenvalues can be obtained by applying DFT to it. It is essentially time-windowing the channel ACF, doing Fourier transform, and sampling the result. Therefore, the faster the channel changes, the narrower the ACF becomes relative to the observation window (the code block length), and a wider Fourier dual

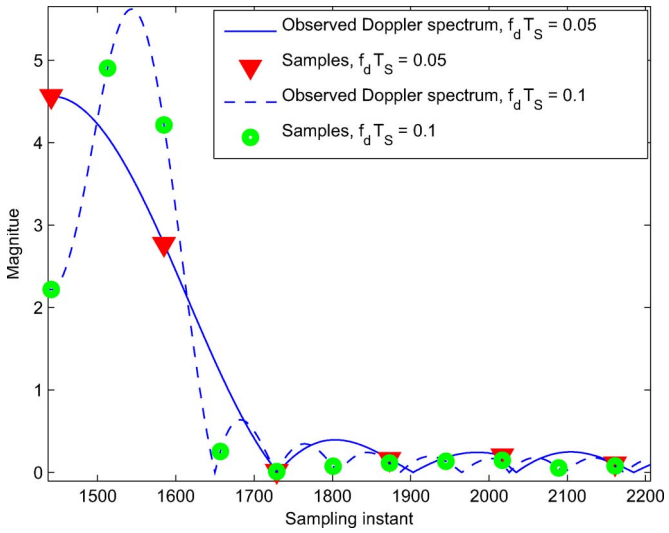

Fig. 3. Eigenvalues are obtained by sampling the convolution of the Doppler spectrum and the sinc function in the frequency domain, which can be recognized as the observed Doppler spectrum. The curves show the effect of different window lengths.

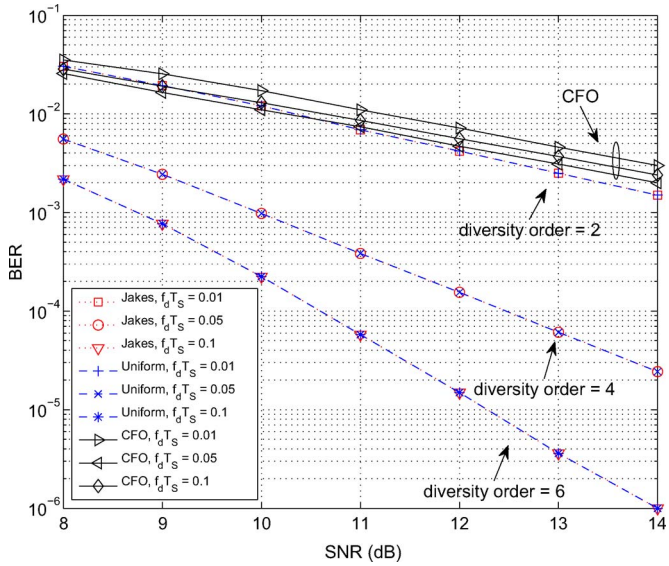

Fig. 4. Comparison of the diversity gain provided by time-varying channels with three kinds of Doppler power spectral density (PSD): Jakes' model, uniform PSD, and CFO. The normalized Doppler frequencies of 0.01, 0.05, and 0.1 are simulated. The path gains $h_p(k;l)$ for different l values are assumed independent. The time variation of the channel $E[h_p(k;l)h_p^*(m;l')]$ is $J_0(2\pi f_d(k-m)T)\cdot\delta(l-l')$ for Jakes' model, $\sin(2\pi f_d(k-m)T)/(\pi(k-m)T)\cdot\delta(l-l')$ for uniform PSD, and $\exp(j2\pi f_d(k-m)T)\cdot\delta(l-l')$ for CFO, where f_d is the maximum Doppler frequency, T is the OFDM sampling time, $J_0(\cdot)$ is the zeroth-order Bessel function of the first kind, and $\delta(\cdot)$ is the Kronecker delta function. Notice that the considered diversity here is the effective diversity order based on the dominant eigenvalues.

and more significant samples follow. Consequently, the diversity order gets larger. Two contrasting examples are shown in Fig. 3, where the observed Doppler spectra are obtained by convolving the Doppler spectra with a sinc function, corresponding to the Fourier transform of time-windowed channel ACFs. After obtaining the observed Doppler spectra, the eigenvalues can be obtained by sampling them.

D. Simulation Results

Back to doubly selective fading channels, Fig. 4 shows the BER performance of a BICM-OFDM system under time-varying channels with two equal-gain paths ($L=2$). The experiments are conducted with three Doppler spectra and different normalized Doppler frequencies. The system uses 8-PSK modulation, the DFT size is 64, $P=10$, and a rate-1/2 convolutional code with the generator polynomial [133; 171] ($d_{\text{free}}=10$) is adopted such that the system performance is not limited by d_{free}. 10^5 channel realizations are simulated. Fig. 4 verifies our predictions on the diversity orders and the effectiveness of the BICM-OFDM systems. For example, by considering the case of Jakes' model with $f_dT_S=0.1$, the six largest eigenvalues of time ACF are 3.96, 3.44, 2.23, 0.349, 0.0162, and 0.0004. The first three eigenvalues contain 99.67% of total channel power. As can be expected, the practical diversity order is limited by $r_T\times L=3\times 2=6$. When f_dT_S is 0.05, the practical diversity order is further reduced to $r_T\times L=2\times 2=4$ since the number of significant eigenvalues of $\mathbf{\Phi}_T$ is cut to 2. The results confirm that larger channel variations lead to higher diversity orders. The case of carrier frequency offset (CFO) is also shown to demonstrate channel variation introduced that does not contribute to diversity. The ACF of this case has $[\mathbf{\Phi}_T]_{k,1:P}=[e^{j2\pi(1-k)f_dT_S},e^{j2\pi(2-k)f_dT_S},\ldots,e^{j2\pi(P-k)f_dT_S}]$ at the kth row. Alternatively, $\mathbf{\Phi}_T$ can be rewritten as $([1,e^{-j2\pi f_dT_S},\ldots,e^{-j2\pi(P-1)f_dT_S}]^T\otimes[1,e^{j2\pi f_dT_S},\ldots,e^{j2\pi(P-1)f_dT_S}])$, which results in a rank-one matrix, and no time diversity gain is available.

Note that, in doing the given simulations, relatively simple channel estimation is required in the sense that only the time-averaged channel within each OFDM symbol needs to be estimated for the receiver to function. The study of channel estimation of OFDM over doubly selective channels has been very active, and many efficient methods are available [4], [13], [20]. Subsequently, efficient ICI cancelation can be done with many methods found in, e.g., [8], [13], and [14].

III. Extension to the Multiple-Input–Multiple-Output Case

The transmission scheme can be extended to MIMO scenarios to benefit from additional gain from spatial diversity. As has been shown, BICM-OFDM can effectively capture time and frequency diversity; to further take advantage of spatial diversity in MIMO situations, a common way is to transform the spatial diversity to time or frequency diversity [11]. In the following, we consider two techniques that achieve this goal with little modifications and overhead cost with respect to BICM-OFDM design for SISO cases. We choose a different approach from the obvious choice of combining BICM-OFDM with space–time coding (STC), which potentially gives an even larger diversity order of $N_T\times\min\{L,d_{\text{free}}\}$ [10], out of the considerations that the simple receivers often used for Alamouti-like schemes suffer greatly in double selective fading environments and the ML decoders for general STC usually carry prohibitively high cost [21]–[23].

A. CDD

The first example is the CDD method used in OFDM systems [24] to transform spatial diversity to multipath diversity (or recognized as frequency diversity), which is done by inserting different cyclic delays to the signal at each transmit antenna. The diversity order is analyzed via the framework established in Section II-B; in essence, the asymptotic diversity order is determined by the rank of $\boldsymbol{R}_{\text{eq}}$. For simplicity, the case of two transmit antennas and one receive antenna is considered, and the results can be extended to more general cases. Starting from the SISO signal model of (2), inserting an intentional delay Δ is equivalent to multiplying a circular shift matrix $\boldsymbol{P}=\begin{bmatrix}\boldsymbol{0} & \boldsymbol{I}_\Delta\\ \boldsymbol{I}_{N-\Delta} & \boldsymbol{0}\end{bmatrix}$ to the transmit signal $\boldsymbol{F}^H\boldsymbol{x}_p$. The receive signal will

be $\boldsymbol{F}\boldsymbol{H}_p\boldsymbol{P}\boldsymbol{F}^H\boldsymbol{x}_p$, and we can combine $\boldsymbol{P}$ and $\boldsymbol{H}_p$ into an equivalent channel. Without loss of generality, assume that an intentional delay Δ is inserted at the second antenna, and (6) is modified for the MIMO case as follows:

$$\boldsymbol{y} = \boldsymbol{X}(\boldsymbol{I}_P \otimes \boldsymbol{F}_{N\times 2L'})\underbrace{(\boldsymbol{h}_1 + \boldsymbol{h}_2)}_{\boldsymbol{h}} + \boldsymbol{z} = \boldsymbol{X}\boldsymbol{h}_{\text{eq}} + \boldsymbol{z} \tag{15}$$

where $L' = L + \Delta$ and $\boldsymbol{h}_1$ and $\boldsymbol{h}_2$ are, respectively, assembled by

$$\begin{aligned}\boldsymbol{h}_1 = \big[&\tilde{h}_1^1(0),\ldots,\tilde{h}_1^1(L-1),\boldsymbol{0}_{1\times\Delta},\tilde{h}_2^1(0),\ldots,\tilde{h}_2^1(L-1),\\ &\boldsymbol{0}_{1\times\Delta},\ldots,\tilde{h}_P^1(0),\ldots,\tilde{h}_P^1(L-1),\boldsymbol{0}_{1\times\Delta}\big]^T_{PL'\times 1}\\ \boldsymbol{h}_2 = \big[&\boldsymbol{0}_{1\times\Delta},\tilde{h}_1^2(0),\ldots,\tilde{h}_1^2(L-1),\boldsymbol{0}_{1\times\Delta},\tilde{h}_2^2(0),\ldots,\\ &\tilde{h}_2^2(L-1),\ldots,\boldsymbol{0}_{1\times\Delta},\tilde{h}_P^2(0),\ldots,\tilde{h}_P^2(L-1)\big]^T_{PL'\times 1}\end{aligned} \tag{16}$$

where superscript is used to denote the transmit antenna index.

Assume that the time and path ACFs of $\boldsymbol{h}_1$ and $\boldsymbol{h}_2$ satisfy the Kronecker model in (9) individually, and denote the spatial correlation matrix between two transmit antennas as $\boldsymbol{\Phi}_S = \begin{bmatrix} 1 & \rho_{12} \\ \rho_{21} & 1 \end{bmatrix}$. Further assume that $L \le \Delta \le N_{\text{cp}} - L$, where N_{cp} is the CP length; then, the taps of $\boldsymbol{h}_1$ and $\boldsymbol{h}_2$ will not overlap in the $\boldsymbol{h}$ in (15), and the length of $\boldsymbol{h}$ of each OFDM symbol is still within N_{cp}. As a result, the autocorrelation matrix of $\boldsymbol{h}$ will satisfy the MIMO Kronecker model as follows:

$$\boldsymbol{R} = E[\boldsymbol{h}\boldsymbol{h}^H] = \boldsymbol{\Phi}_T \otimes \boldsymbol{\Phi}_S \otimes \boldsymbol{\Phi}_L, \tag{17}$$

and thus

$$\text{rank}(\boldsymbol{R}_{\text{eq}}) = r_T \times N_T \times L. \tag{18}$$

Following the approach in Section II-B, it is straightforward to see from (18) that the maximum achievable diversity order is $\min\{r_T \times N_T \times L, d_{\text{free}}\}$. Fig. 5 shows the BER performance of a MIMO BICM-OFDM system employing CDD with the normalized Doppler frequency set to 0.05. (Thus, r_T is 2.) The slopes coincide with the analysis results, and the diversity order increases with the path and antenna counts.

B. PRD

The second example is to generalize the phase-roll scheme [11], in which the correlation function of the equivalent channel $h[k] = h_1 + h_2 e^{j2\pi k\theta}$ has zeros at certain delays, i.e., $R_k[\Delta k] = (1/2)E\{h[k]h^*[k+\Delta k]\} = (1/2)(1+e^{j2\pi\Delta k\theta}) = 0$ at $\Delta k\theta = (1/2), (3/2), (5/2), \ldots$. Zero correlation, as demonstrated in Section II-B, in turn implies independent channel conditions and opportunities to exploit diversity. One interesting scenario happens when multiple CFOs exist among collaborating transmitters in cooperative communications. The scenario can be fitted into a PRD model with unintentional phase differences induced by CFOs. We have reported simulation results of similar schemes in [12] in which the effectiveness of PRD is clearly demonstrated.

Similarly as in the CDD case, by combining the phase rotation matrix $\boldsymbol{E} = \text{diag}(1, e^{j(2\pi\varepsilon/N)}, \ldots, e^{j(2\pi\varepsilon(N-1)/N)})$ and $\boldsymbol{H}_p$ into an equivalent channel, (6) can be rewritten as (when there are two transmit antennas)

$$\boldsymbol{y} = \boldsymbol{X}(\boldsymbol{I}_P \otimes \boldsymbol{F}_{N\times L})(\boldsymbol{E}_1\boldsymbol{h}_1 + \boldsymbol{E}_2\boldsymbol{h}_2) + \boldsymbol{z} = \boldsymbol{X}\boldsymbol{h}_{\text{eq}} + \boldsymbol{z} \tag{19}$$

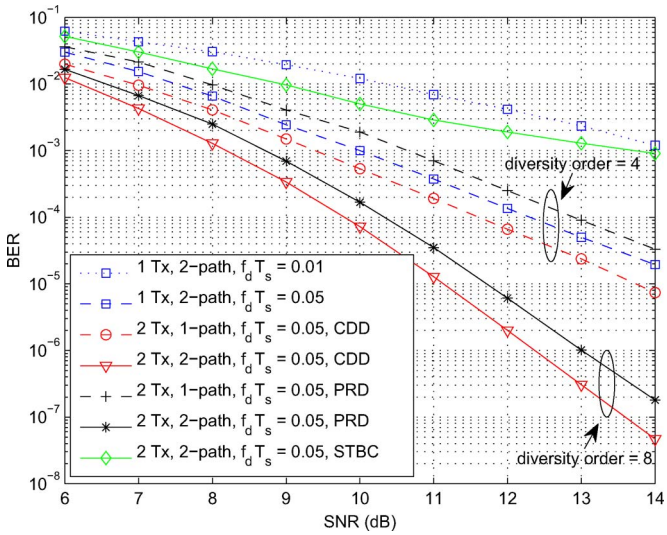

Fig. 5. BER comparison of the MIMO BICM-OFDM employing CDD, PRD, and STBC over doubly selective fading channels. The DFT size is 64, $P = 10$, and a rate-1/2 convolutional code with the generator polynomial [133; 171] ($d_{\text{free}} = 10$) is adopted. Notice that the considered diversity here is the effective diversity order based on the dominant eigenvalues. The channel is the equal-gain dual path at $l = 0$ and $l = 1$, and the introduced cyclic delay Δ is 5. The parameters of PRD are chosen as $\varepsilon_1 = 0.05$ and $\varepsilon_2 = -0.05$.

where $\boldsymbol{E}_\alpha = \text{diag}([1,1,\ldots,1] \otimes [e^{j(2\pi\varepsilon_\alpha(N-1)/2/N)}, e^{j(2\pi\varepsilon_\alpha 2(N-1)/2/N)}, \ldots, e^{j(2\pi\varepsilon_\alpha P(N-1)/2/N)}])$, $\alpha \in \{1,2\}$, is a $PL \times PL$ diagonal matrix representing phase offsets; and $\boldsymbol{h}_\alpha$ is defined as

$$\begin{aligned}\boldsymbol{h}_\alpha = \big[&\tilde{h}_1^\alpha(0),\ldots,\tilde{h}_1^\alpha(L-1),\tilde{h}_2^\alpha(0),\ldots,\tilde{h}_2^\alpha(L-1)\\ &\ldots,\tilde{h}_P^\alpha(0),\ldots,\tilde{h}_P^\alpha(L-1)\big]^T_{PL\times 1}.\end{aligned} \tag{20}$$

Assume that we correct the phase offset from the first transmit antenna; thus, $\boldsymbol{E}_1$ becomes an identity matrix. The rank of $\boldsymbol{R}_{\text{eq}}$ can be bounded by [19, Fact 2.10.7]

$$\begin{aligned}\text{rank}(\boldsymbol{R}_{\text{eq}}) &= \text{rank}\left(\boldsymbol{R} + \boldsymbol{E}_2\boldsymbol{R}\boldsymbol{E}_2^H\right)\\ &\le \text{rank}(\boldsymbol{R}) + \text{rank}\left(\boldsymbol{E}_2\boldsymbol{R}\boldsymbol{E}_2^H\right) = r_T \times L \times 2.\end{aligned} \tag{21}$$

The last equation follows that $\text{rank}(\boldsymbol{R}) = \text{rank}(\boldsymbol{E}_2\boldsymbol{R}\boldsymbol{E}_2^H) = r_T \times L$. The maximum diversity order is increased by N_T due to space diversity if d_{free} is not the limiting factor. Although the analysis does not find the condition when the bound can be achieved, simulation results, such as those shown in Fig. 5, indicate that it is achievable.

For slow fading channels, it is worth noting that, in [17], the diversity gain provided by multiple transmit antennas appears in the same form as our result. However, it is not surprising since both methods transform spatial diversity into other types of diversity for easier harvest. Finally, the simulation results show the weakness of the Alamouti scheme over doubly selective fading channels. Consider the example of space–time Alamouti code where the signal matrix $\boldsymbol{X}$ in (6) becomes $\text{diag}(\boldsymbol{X}_1^{ST}, \ldots, \boldsymbol{X}_{P/2}^{ST})$, where $\boldsymbol{X}_p^{ST} = \begin{bmatrix} \boldsymbol{X}_{2(p-1)+1} & \boldsymbol{X}_{2(p-1)+2} \\ -\boldsymbol{X}_{2(p-1)+2}^H & \boldsymbol{X}_{2(p-1)+1}^H \end{bmatrix}$ with $\boldsymbol{X}_p = \text{diag}(X((p-1)N), X((p-1)N+1), \ldots, X((p-1)N+N-1))$. One would expect the diversity order to be $P \times \min\{L, d_{\text{free}}\}$; however, the performance degrades severely, and an error floor occurs if a typical Alamouti receiver is deployed. The degradation is caused by channel variations within an Alamouti code word and the induced destruction of the Alamouti structure.

IV. Conclusion

In this paper, the diversity orders of BICM-OFDM over doubly selective fading channels have been examined for both the asymptotic condition of very high SNR and the realistic situation with moderate SNRs. It is shown by simulation that the later diversity order is practically governed by dominant eigenvalues of the channel ACF. The same analysis framework is extended to show that BICM-OFDM, together with MIMO techniques, can provide even higher diversity gains in, e.g., in asynchronous cooperative communications. The results provide insights into the design/tradeoff of design parameters of BICM-OFDM systems, e.g., the achievable time diversity order versus the length of blocks.

Acknowledgment

The authors thank Prof. D. W. Lin of NCTU and the anonymous reviewers for their careful reading and helpful guidance.

References

[1] G. Caire, G. Taricco, and E. Biglieri, "Bit-interleaved coded modulation," *IEEE Trans. Inf. Theory*, vol. 44, no. 3, pp. 927–946, May 1998.
[2] X. Li, A. Chindapol, and J. A. Ritcey, "Bit-interleaved coded modulation with iterative decoding and 8 PSK signaling," *IEEE Trans. Commun.*, vol. 50, no. 8, pp. 1250–1257, Aug. 2002.
[3] W. G. Jeon, K. H. Chang, and Y. S. Cho, "An equalization technique for orthogonal frequency-division multiplexing systems in time-variant multipath channels," *IEEE Trans. Commun.*, vol. 47, no. 1, pp. 27–32, Jan. 1999.
[4] Y. S. Choi, P. J. Voltz, and F. A. Cassara, "On channel estimation and detection for multicarrier signals in fast and selective Rayleigh fading channels," *IEEE Trans. Commun.*, vol. 49, no. 8, pp. 1375–1387, Aug. 2001.
[5] X. Cai and G. B. Giannakis, "Bounding performance and suppressing intercarrier interference in wireless mobile OFDM," *IEEE Trans. Commun.*, vol. 51, no. 12, pp. 2047–2056, Dec. 2003.
[6] P. Schniter, "Low-complexity equalization of OFDM in doubly selective channels," *IEEE Trans. Signal Process.*, vol. 52, no. 4, pp. 1002–1011, Apr. 2004.
[7] X. Ma and G. Giannakis, "Maximum-diversity transmissions over doubly selective wireless channels," *IEEE Trans. Inf. Theory*, vol. 49, no. 7, pp. 1832–1840, Jul. 2003.
[8] D. Huang, K. B. Letaief, and J. Lu, "Bit-interleaved time–frequency coded modulation for OFDM systems over time-varying channels," *IEEE Trans. Commun.*, vol. 53, no. 7, pp. 1191–1199, Jul. 2005.
[9] D. N. Liu and M. P. Fitz, "Iterative MAP equalization and decoding in wireless mobile coded OFDM," *IEEE Trans. Commun.*, vol. 57, no. 7, pp. 2042–2051, Jul. 2009.
[10] E. Akay and E. Ayanoglu, "Achieving full frequency and space diversity in wireless systems via BICM, OFDM, STBC, and Viterbi decoding," *IEEE Trans. Commun.*, vol. 54, no. 12, pp. 2164–2172, Dec. 2006.
[11] A. Paulraj, R. Nabar, and D. Gore, *Introduction to Space-Time Wireless Communications*. Cambridge, U.K.: Cambridge Univ. Press, 2003.
[12] H.-D. Lin, T.-H. Sang, and D. W. Lin, "BICM-OFDM for cooperative communications with multiple synchronization errors," in *Proc. Int. Wireless Commun. Mobile Comput. Conf.*, Jul. 2010, pp. 1055–1059.
[13] A. Gorokhov and J. P. Linnartz, "Robust OFDM receivers for dispersive time-varying channels: Equalization and channel acquisition," *IEEE Trans. Commun.*, vol. 52, no. 4, pp. 572–583, Apr. 2004.
[14] Y. Mostofi and D. C. Cox, "ICI mitigation for pilot-aided OFDM mobile systems," *IEEE Trans. Wireless Commun.*, vol. 4, no. 2, pp. 765–774, Mar. 2005.
[15] *Wireless LAN Medium Access Control (MAC) and Physical Layer (PHY) specifications: High-speed Physical Layer in the 5 GHz Band*, IEEE Std. 802.11a, 1999.
[16] D. Tse and P. Viswanath, *Fundamentals of Wireless Communication*, 1st ed. Cambridge, U.K.: Cambridge Univ. Press, 2005.
[17] H. Z. B. Chen and R. Schober, "Cyclic space-frequency filtering for BICM-OFDM systems with multiple co-located or distributed transmit antennas," *IEEE Trans. Wireless Commun.*, vol. 8, no. 4, pp. 1825–1835, Apr. 2009.
[18] H. Z. B. Chen, R. Schober, and W. Gerstacker, "Robust transmit processing for BICM-OFDM systems," *IEEE Trans. Wireless Commun.*, vol. 8, no. 11, pp. 5671–5681, Nov. 2009.
[19] D. S. Bernstein, *Matrix Mathematics: Theory, Facts, and Formulas*, 2nd ed. Princeton, NJ: Princeton Univ. Press, 2009.
[20] T. Y. Al-Naffouri, K. M. Z. Islam, N. Al-Dhahir, and S. Lu, "A model reduction approach for OFDM channel estimation under high mobility conditions," *IEEE Trans. Signal Process.*, vol. 58, no. 4, pp. 2181–2193, Apr. 2010.
[21] J. Kim, R. W. Heath, Jr., and E. J. Powers, "Receiver designs for Alamouti coded OFDM systems in fast fading channels," *IEEE Trans. Wireless Commun.*, vol. 4, no. 2, pp. 550–559, Mar. 2005.
[22] S. Lu, B. Narasimhan, and N. Al-Dhahir, "A novel SFBC-OFDM scheme for doubly selective channels," *IEEE Trans. Veh. Technol.*, vol. 58, no. 5, pp. 2573–2578, Jun. 2009.
[23] D.-B. Lin, P.-H. Chiang, and H.-J. Li, "Performance analysis of two-branch transmit diversity block-coded OFDM systems in time-varying multipath Rayleigh-fading channels," *IEEE Trans. Veh. Technol.*, vol. 54, no. 1, pp. 136–148, Jan. 2005.
[24] J. Tan and G. L. Stüber, "Multicarrier delay diversity modulation for MIMO systems," *IEEE Trans. Wireless Commun.*, vol. 3, no. 5, pp. 1756–1763, Sep. 2004.

On the Design of Amplify-and-Forward MIMO-OFDM Relay Systems With QoS Requirements Specified as Schur-Convex Functions of the MSEs

Luca Sanguinetti, *Member, IEEE*, Antonio A. D'Amico, and Yue Rong, *Senior Member, IEEE*

***Abstract*—In this paper, we focus on the design of linear and nonlinear architectures in amplify-and-forward multiple-input–multiple-output (MIMO) orthogonal frequency-division multiplexing (OFDM) relay networks in which different types of services are supported. The goal is to jointly optimize the processing matrices to minimize the total power consumption while satisfying the quality-of-service (QoS) requirements of each service specified as Schur-convex functions of the mean square errors (MSEs) over all assigned subcarriers. It turns out that the optimal solution leads to the diagonalization of the source–relay–destination channel up to a unitary matrix, depending on the specific Schur-convex function.**

***Index Terms*—Amplify-and-forward, multiple-input multiple-output (MIMO), nonregenerative relay, orthogonal frequency-division multiplexing (OFDM), power minimization, quality-of-service (QoS) requirements, Schur-convex functions, transceiver design.**

I. Introduction

Over the past few years, the ever-increasing demand for high-speed ubiquitous wireless communications has motivated an intense research activity toward the development of transmission technologies characterized by high spectral efficiency and high reliability. The most promising solutions in this direction rely on orthogonal frequency-division multiplexing (OFDM) techniques, multiple-input–multiple-

Manuscript received July 23, 2012; accepted December 18, 2012. Date of publication December 25, 2012; date of current version May 8, 2013. The review of this paper was coordinated by Dr. T. Jiang.

L. Sanguinetti and A. A. D'Amico are with the Department of Information Engineering, University of Pisa, 56126 Pisa, Italy (e-mail: luca.sanguinetti@iet.unipi.it; a.damico@iet.unipi.it).

Y. Rong is with the Department of Electrical and Computer Engineering, Curtin University of Technology, Bentley, WA 6102, Australia (e-mail: y.rong@curtin.edu.au).

Color versions of one or more of the figures in this paper are available online at http://ieeexplore.ieee.org.

Digital Object Identifier 10.1109/TVT.2012.2236370